J Mater Sci: Mater Electron (2013) 24:4439–4444
DOI 10.1007/s10854-013-1422-9

Deposition of Cu–Mn alloy film from supercritical carbon dioxide for advanced interconnects

Bin Zhao · Yanfei Zhang · Junhe Yang

Received: 24 June 2013 / Accepted: 27 July 2013 / Published online: 8 August 2013

Abstract Cu–Mn alloy films for microelectronic interconnects were deposited by H_2 reduction of bis(2,2,6,6-tetramethyl-3,5-heptanedionato)-copper(II) [$Cu(tmhd)_2$] and bis(penta-methylcyclopentadienyl)-manganese [$Mn(pmcp)_2$] in supercritical carbon dioxide ($scCO_2$). 20-nm thick and continuous Cu–Mn films with a smooth surface were deposited at the temperature of 210 °C. Manganese was found to be segregated to film surface and its content on the surface increased with increasing Mn precursor concentration in $scCO_2$. Mn addition by supercritical fluid deposition could improve surface quality of the Cu film. And electrical resistivity of the Cu–Mn films increased with the Mn contents in the film.

1 Introduction

Cu has been used as an interconnect material over Al in ultra-large-scale-integration (ULSI) and micro-electro-mechanical systems (MEMS) because of its low electrical resistivity and high electromigration (EM) resistance [1, 2]. However, the introduction of Cu also leads to some new reliability issues. In actual Cu interconnects, the fast diffusion path of EM is the interfaces between Cu metal and a dielectric cap or barrier layer, rather than grain boundaries [3]. Therefore, EM is still a significant reliability problem for Cu metallization. It was reported that the EM lifetime of Cu interconnects can be improved by using a metallic cap or inserting an adhesion promoter between Cu and diffusion barrier [4, 5]. When the interface diffusion is effectively suppressed, grain-boundary diffusion may turn into the main EM mechanism [6]. Alloying has been proved to be a promising technique to retard grain-boundary EM, since the alloy element reduces the drift velocity of Cu atoms by segregating at grain boundaries and interfaces [7]. Thus far, a number of dilute Cu alloys have been investigated for interconnects application, such as Cu–Al, and Cu–Sn [8, 9]. However, these alloy elements usually lead to a significant increase in Cu resistivity, which is the dominant drawback of using Cu alloys in microelectronic metallization [10].

The ideal alloy element should lead to enhanced EM resistance by segregating to the fast diffusion path without significantly increasing the resistance of interconnects. Since the activity coefficient of Mn in Cu is larger than 1 [11], Mn can be easily expelled from Cu and segregated to interfaces and grain boundaries during annealing [11, 12]. Au et al. [13] found that the resistivity of Cu–Mn seed layer could approach that of pure Cu film with the same thickness after annealing. Therefore, Cu–Mn alloy may be a promising candidate material for highly reliable interconnects. It is well established that doping seed layer is the most feasible way to realize integration of Cu alloys into the standard damascene process. However, with aggressively shrinking of feature size, it will be more and more challenging to fabricate a continuous and ultrathin Cu seed layer by conventional physical vapor deposition (PVD) method [14].

Recently, supercritical fluid deposition (SCFD) was introduced to prepare Cu seed layer and exhibited excellent gap-filling and step-coverage capabilities [15, 18]. SCFD is a novel deposition method in which chemical reagents react to form thin films in supercritical carbon dioxide ($scCO_2$) [15]. The benefit of SCFD over conventional deposition techniques lies in the unique properties of

B. Zhao · Y. Zhang · J. Yang (✉)
School of Materials Science and Engineering, University of Shanghai for Science and Technology, Shanghai 200093, China
e-mail: jhyang@usst.edu.cn

$scCO_2$. Specifically, the gas-like diffusivity enables fast precursor supply leading to conformal deposition into narrow spaces [16, 17]. And the liquid-like solubility of $scCO_2$ accomplishes deposition with high precursor concentration, which has a potential for making aggressive use of various types of precursor and to realize high-density nucleation [17, 18]. Although a number of metal films have been prepared using SCFD, including Cu, Ni, Ru, Au, Ag [15–18], the deposition of thin and smooth Cu alloy seed layer by this technique was still worth investigating. In this study, we demonstrate the feasibility of Cu–Mn alloy film deposition from $scCO_2$. Effects of temperature and Mn precursor content in $scCO_2$ on morphology, surface quality and composition of Cu–Mn films were investigated.

2 Experimental

Bis(2,2,6,6-tetramethyl-3,5-heptanedionato)copper(II) [Cu $(tmhd)_2$] and bis (pentamethylcyclopentadienyl)-manganese [$Mn(pmcp)_2$] were used as the copper and manganese precursors, respectively. High purity CO_2 (+99.999 %) and H_2 (+99.999 %) were used in the experiments. The substrate employed were Si wafers with an 80 nm Ru surface layer sputtered at 400 °C, as Ru is a promising candidate material for adhesion promoter on diffusion barrier [19].

The deposition was carried out in a hot-wall batch reactor. Figure 1 shows a schematic diagram of the SCFD apparatus used in this study. It consists of a high pressure syringe pump, a 30-mL stainless steel reactor and a separator. In typical experiments, a 2 × 2 cm^2 substrate was mounted on the bottom of the reactor, and a predetermined amount of Cu precursor and Mn precursor were loaded in a N_2-filled glovebox since $Mn(pmcp)_2$ is air sensitive. Then the reactor was sealed and preheated to 50 °C. After that, H_2 was introduced to the reactor at 2 MPa and CO_2 was pressurized to 10 MPa using a high-pressure syringe pump. Subsequently, the reactor was heated to desired temperature (180–210 °C) at a rate of 7–8 °C/min and maintained for 30 min. Finally, the heating power was turned off and the reactor effluent was vented. For all the experiments, the Cu precursor concentration in $scCO_2$ was kept at 1.0 mmol/L and Mn precursor concentration varied between 0.033 and 0.33 mmol/L. Excess H_2 over the metal precursors was used for the deposition and H_2 concentration in $scCO_2$ was 0.75 mol/L.

Surface morphology of the deposited films was observed using field emission scanning electron microscopy (FE-SEM; Quanta FEG450) and atomic force microscopy (AFM; SHIMADZU SPM-9500J3). Root mean square (RMS) values obtained from AFM analysis of 5 × 5 μm^2 area were used to determine the surface roughness of the films. The chemical composition was analyzed using X-ray photoelectron spectroscopy (XPS; Perkin Elmer HP1500). Electrical resistivity of the films was calculated from the sheet resistance measured with a four-point probe method.

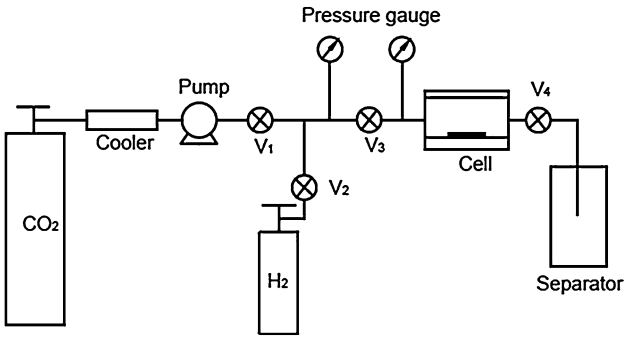

Fig. 1 Schematic diagram of the hot-wall batch system for SCFD

3 Results and discussion

The effect of temperature on Cu–Mn film deposition was first investigated. Cu precursor of 1.0 mmol/L and Mn precursor of 0.33 mmol/L were utilized for the deposition. Figure 2 shows surface morphologies of the films deposited at temperatures ranging between 180 and 210 °C. When Cu and Mn precursors were introduced with H_2 at 180 °C, a discontinuous film was obtained, and some partially-connected clusters was observed on Ru substrate, as shown in Fig. 2a. With increasing the temperature, the clusters were further coalesced to form a denser film. However, a close examination revealed that there were still some pinholes in the films when deposited at 190 and 200 °C (Fig. 2b, c). When the temperature was increased to 210 °C, a 20-nm-thick dense film was observed on Ru surface (Fig. 2d). The film was further analyzed using XPS. And no signals of Ru appeared in the survey spectra (not shown here), suggesting that the substrate was covered by a continuous layer, which confirms the continuity of the Cu–Mn film obtained at 210 °C.

Figure 3 shows high-resolution XPS spectra of the Cu–Mn film deposited at 210 °C after Ar^+ sputtering. The Cu $2p_{1/2}$ and Cu $2p_{3/2}$ peaks at 952.7 and 932.9 eV, as well as the binding energy difference between these two peaks, 19.8 eV, indicate that the film is composed of metallic Cu (Fig. 3a). And the appearance of Mn $2p_{1/2}$ and $2p_{3/2}$ peaks also suggests the presence of Mn in the film (Fig. 3b). After removing surface contaminants by sputtering, oxygen impurity less than 0.58 at.% was detected in the film (Fig. 3c), and the level of carbon in the bulk of the sample was below the instrument detection limit (Fig. 3d), indicating the high purity of the Cu–Mn alloy film. It is worth noting that, a small amount of oxygen was still detected in the film despite of the presence of H_2. Possibly, trace water

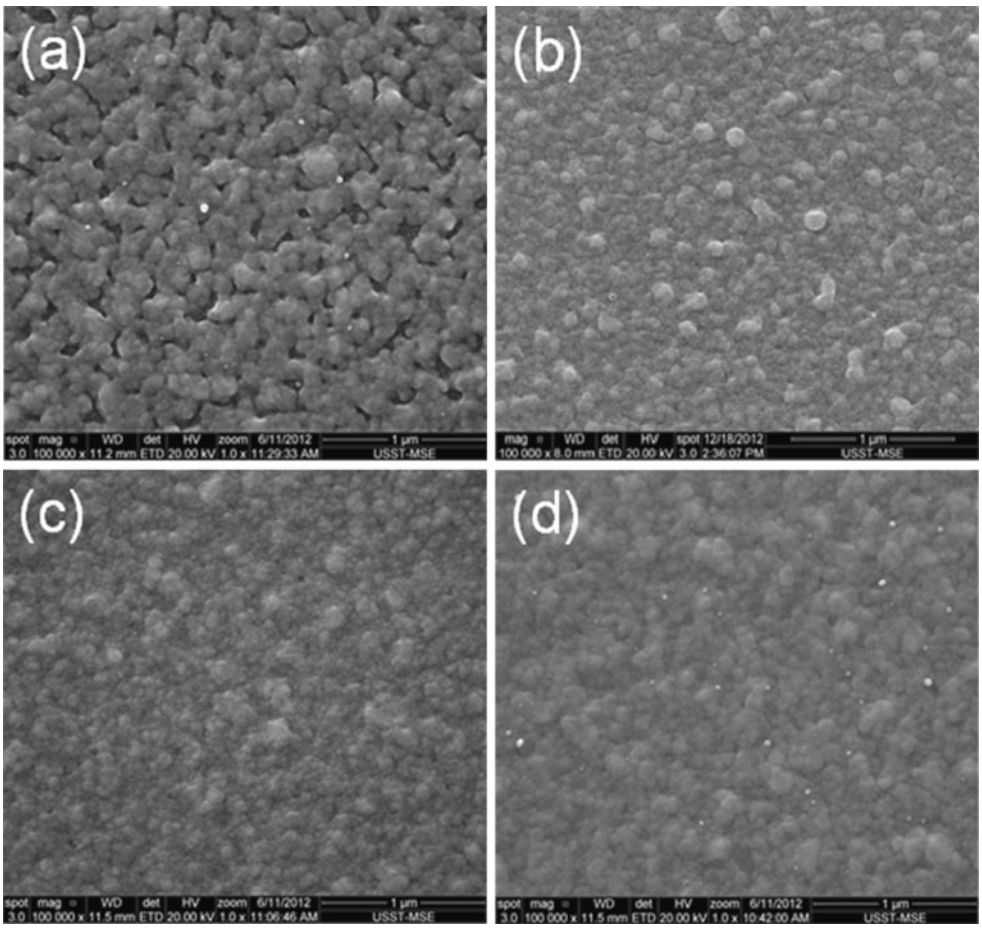

Fig. 2 SEM images of the Cu–Mn alloy films deposited on Ru substrate from 1.0 mmol/L $Cu(tmhd)_2$ and 0.33 mmol/L $Mn(pmcp)_2$ at the temperature: **a** 180 °C, **b** 190 °C, **c** 200 °C, and **d** 210 °C

impurity in CO_2 acted as the oxidant because Mn is extremely easily oxidized and the MnO_x cannot be reduced by H_2 [20].

Since a dilute alloy is usually desired for Cu interconnects, we attempted to reduce Mn contents in the alloy films by decreasing the concentration of $Mn(pmcp)_2$ in $scCO_2$, while keeping the amount of Cu precursor constant. After deposition, XPS was carried out to examine the Mn content on the film surface. When 0.33 mmol/L $Mn(pmcp)_2$ was loaded together with the Cu precursor, the atomic concentration of Mn was found to be around 33 at.%. Unexpectedly, decreasing the $Mn(pmcp)_2$ concentration 10 times to 0.033 mmol/L, the alloying content did not drop significantly, and 25.7 at.% Mn was detected on the film surface. Figure 4 shows the Mn content dependence on the precursor concentration in $scCO_2$. The Mn content in the film was somehow affected by Mn precursor concentration, but there is not a proportional scaling relationship between them. Insufficient solubility of the Mn precursor in $scCO_2$ may be one of the reasons for this discrepancy. Although we did not intend to quantify the solubility of $Mn(pmcp)_2$ in $scCO_2$, a portion of the Mn precursor was found to remain in the reactor after deposition when the concentration of over 0.1 mmol/L was used. The nonlinear dependence of Mn deposition rate on the precursor concentration is also a possible reason, which needs further investigation in the future. Besides, it was found that, even though the Cu/Mn precursor ratio of 30/1 was used, the Cu/Mn atomic proportion on the film surface was still close to 3/1. Therefore, we believed that the Mn was concentrated in the surface area rather than distributed evenly in the film, possibly attributed to the higher thermal stability of $Mn(pmcp)_2$ than that of $Cu(tmhd)_2$ [21].

Influence of Mn precursor concentration on surface roughness of the Cu–Mn films was also investigated. Figure 5 presents the AFM images of the pure Cu and Cu–Mn films prepared using different Mn precursor concentration. Considering the low solubility of Mn precursor in $scCO_2$ and the identical Cu precursor concentration used for all the experiments, the alloy film thickness was regarded as constant. Interestingly, the surface quality of Cu–Mn alloy film was found to be improved by adding more Mn

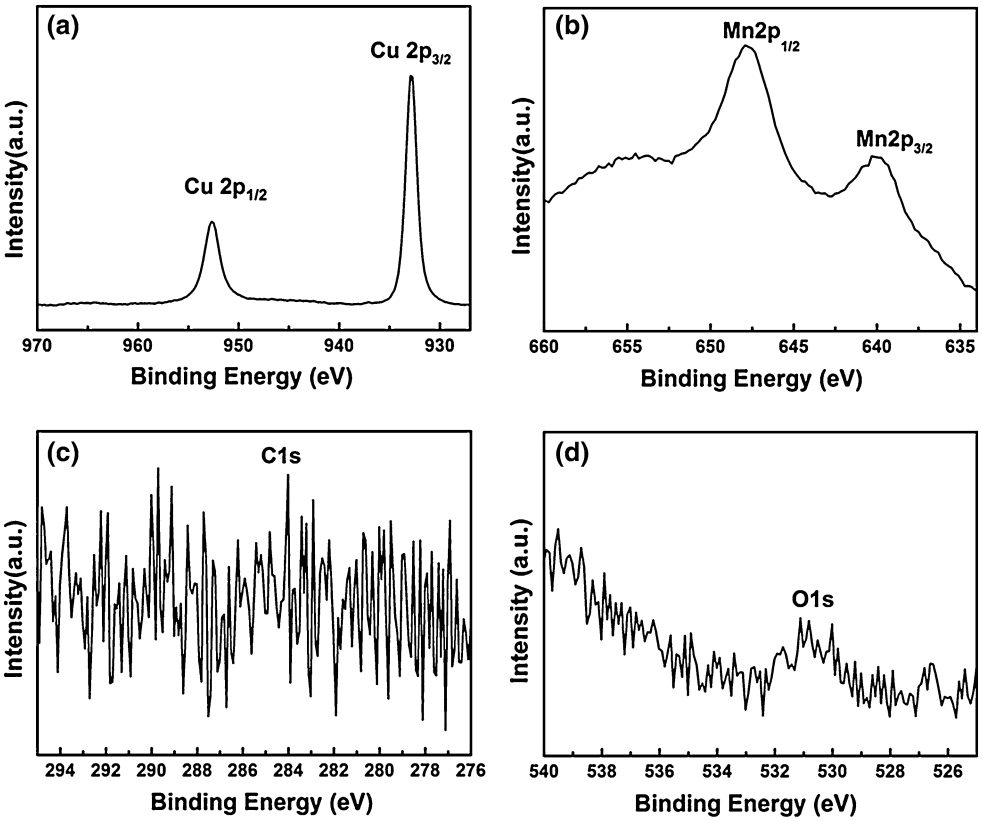

Fig. 3 High-resolution XPS spectra of: **a** Cu 2p, **b** Mn 2p, **c** C 1 s, and **d** O 1 s, for the Cu–Mn alloy film deposited from 1.0 mmol/L $Cu(tmhd)_2$ and 0.33 mmol/L $Mn(pmcp)_2$ at 210 °C

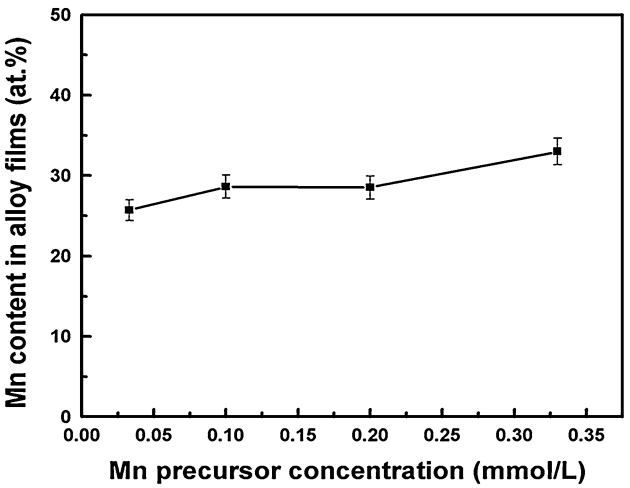

Fig. 4 Mn content dependence on the precursor concentration in $scCO_2$

precursor. And the RMS surface roughness decreased from 7.1 nm for the pure Cu film to 3.0 nm when 0.33 mmol/L $Mn(pmcp)_2$ was utilized.

Electrical resistivities of the Cu–Mn alloy films were measured by four-point probe method and found to range between 3.7 and 5.7 μΩ-cm. Figure 6 shows the film resistivity as a function of the Mn precursor concentration. It is worth noting that the resistivity of the 20-nm thick Cu film was about 3.7 μΩ-cm, much higher than the resistivity of bulk Cu, which is due to the size effect resulting from surface scattering and grain-boundary scattering [22]. Obviously, as the $Mn(pmcp)_2$ concentration in $scCO_2$ increased, the resistivity of Cu–Mn film increased accordingly. The worsening in electrical conductivity of the film could be attributed to the increased Mn content in the films. A comparison between Figs. 4, 6 showed a noticeable difference in increment extent of the Mn content and the film resistivity with the Mn precursor concentration. This indicated that a small amount of Mn was deposited in the bulk film and the Mn content in the bulk film increased with raising Mn precursor concentration in $scCO_2$. Based on this and the previous inference that most Mn was concentrated in the film surface, possible mechanism for Mn deposition was interpreted as follows. Due to the limited solubility of Mn precursor in $scCO_2$, nucleation and growth of the Mn layer was quite slow. So, only small amount of Mn was deposited in the film together with Cu during heating. When the temperature reached 210 °C, most Cu precursor had been consumed [23], and thus Mn was deposited slowly on the film surface while maintaining temperature. Although the solubility of Mn precursor was limited, the actual precursor concentration in $scCO_2$ did increase slightly with loading more Mn precursor. Therefore, the nucleation density and growth rate of Mn

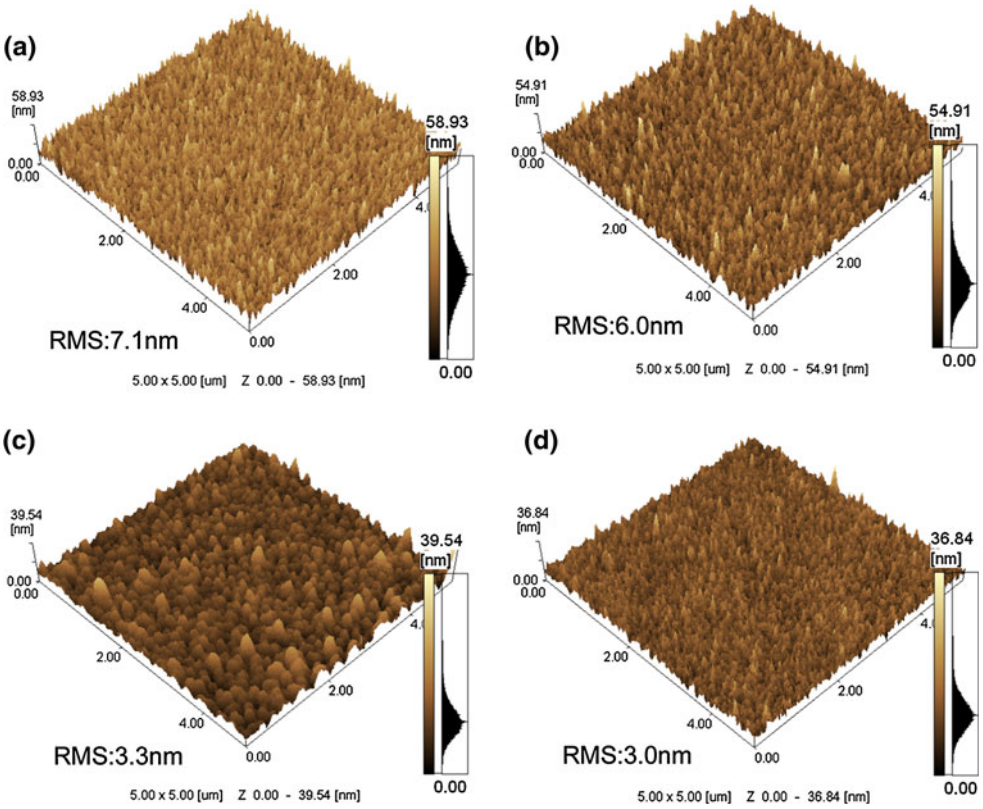

Fig. 5 AFM images of **a** the Cu film deposited from 1.0 mmol/L $Cu(tmhd)_2$, and the Cu–Mn alloy films deposited from 1.0 mmol/L $Cu(tmhd)_2$ and the Mn precursor of: **b** 0.03 mol/L, **c** 0.2 mol/L, **d** 0.3 mol/L

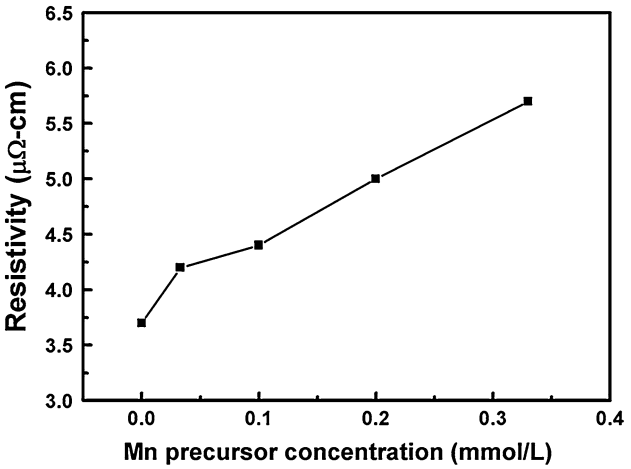

Fig. 6 Film resistivity as a function of the Mn precursor concentration

increased accordingly, similar to the tendency reported for Cu [23], which might lead to the increased Mn content in the bulk films. On the other hand, some Mn atoms on the surface could also diffuse into the bulk film through grain boundaries during maintaining the temperature. Both the increase of Mn contents on the film surface and in the bulk film contributed to the increment of the film resistivity. Therefore, to make a Cu–Mn seed layer with low resistivity, the Mn content should be well controlled.

4 Conclusion

Cu–Mn alloy films were prepared on Ru substrate by co-deposition of $Cu(tmhd)_2$ and $Mn(pmcp)_2$ in $scCO_2$. Deposition at temperature below 200 °C did not yield continuous film and a dense alloy film of 20 nm was successfully deposited at 210 °C. By reducing the Mn precursor concentration from 0.33 to 0.033 mmol/L while maintaining the Cu precursor amount, the Mn content in the alloy film decreased. And Mn was found to be concentrated in the film surface, possibly attributed to the higher thermal stability of the Mn precursor than $Cu(tmhd)_2$. It was found that the Mn alloying by SCFD could improve surface roughness of the Cu film, but the film resistivity also rose with increasing the alloying content. SCFD was proved to be a promising technique for deposition of thin and smooth Cu alloy seed layers.

Acknowledgments The authors gratefully acknowledge financial support from NSFC (50901086 and 51072118), Science Foundation for the Excellent Youth Scholars of Shanghai Municipal Education Commission (slg10032), Qianjiang Project of Zhejiang Province (2010R10047), and SRF for ROCS, SEM.

References

1. S.P. Murarka, Multilevel interconnections for ULSI and GSI era. Mater. Sci. Eng. R **19**, 87–151 (1997)

2. M. Hansan, J.F. Rohan, Cu electrodeposition from methanesulfonate electrolytes for ULSI and MEMS applications. J. Electrochem. Soc. **157**, D278–D282 (2010)
3. K.N. Tu, Recent advances on electromigration in very-large-scale-integration of interconnects. J. Appl. Phys. **94**, 5451–5473 (2003)
4. C.C. Yang, P. Flaitz, B. Li, F. Chen, C. Christiansen, S.Y. Lee, P. Ma, D. Edelstein, Co capping layers for Cu/low-k interconnects. Microelectron. Eng. **92**, 79–82 (2012)
5. H. Kim, T. Koseki, T. Ohba, T. Ohta, Y. Kojima, H. Sato, Y. Shimogaki, Cu wettability and diffusion barrier property of Ru thin film for Cu metallization. J. Electrochem. Soc. **152**, G594–G600 (2005)
6. L. Zhang, M. Kraatz, O. Aubel, C. Hennesthal, J. Im, E. Zschech, P.S. Ho, in *Proceedings of the IEEE 2010 International Interconnect Technology Conference (IITC 2010)*, 2010, p. 1
7. B. Zhao, T. Momose, Y. Shimogaki, Deposition of Cu–Ag alloy film by supercritical fluid deposition. Jpn. J. Appl. Phys. **45**, L1296–L1299 (2006)
8. S. Muranaka, M. Sueyoshi, K. Mori, K. Maekawa, M. Fujisawa, K. Asai, Effect of impurities and microstructure of Cu electroplated film on reliability of Cu interconnects using CuAl alloy seed. Microelectron. Eng. **105**, 91–94 (2013)
9. I. Volov, X. Sun, G. Gadikota, P. Shi, A.C. West, Electrodeposition of copper–tin film alloys for interconnect applications. Electrochim. Acta **89**, 792–797 (2013)
10. K. Barmak, A. Gungor, C. Cabral, J.M.E. Harper, Annealing behavior of Cu and dilute Cu-alloy films: precipitation, grain growth, and resistivity. J. Appl. Phys. **94**, 1605–1616 (2003)
11. J. Koike, M. Wada, Self-forming diffusion barrier layer in Cu–Mn alloy metallization. Appl. Phys. Lett. **87**, 041911–041913 (2005)
12. M.H. Lin, A.S. Oates, Electromigration in dual-damascene CuMn alloy IC interconnects. IEEE Trans. Device Mat. R. **13**, 330–332 (2013)
13. Y. Au, Q.M. Wang, H. Li, J.M. Lehn, D.V. Shenai, R.G. Gordon, Vapor deposition of highly conformal copper seed layers for plating through-silicon vias (TSVs). J. Electrochem. Soc. **159**, D382–D385 (2012)
14. S. Armini, Z. El-Mekki, K. Vandersmissen, H. Philipsen, S. Rodet, M. Honore, A. Radisic, Y. Civale, E. Beyne, L. Leunissen, Void-free filling of HAR TSVs using a wet alkaline Cu seed on CVD Co as a replacement for PVD Cu seed. J. Electrochem. Soc. **158**, H160–H165 (2011)
15. J.M. Blackburn, D.P. Long, A. Cabanas, J.J. Watkins, Deposition of conformal copper and nickel films from supercritical carbon dioxide. Science **294**, 141–145 (2001)
16. C.F. Karanikas, J.J. Watkins, Kinetics of the ruthenium thin film deposition from supercritical carbon dioxide by the hydrogen reduction of $Ru(tmhd)_2cod$. Microelectron. Eng. **87**, 566–572 (2010)
17. A. Cabanas, D.P. Long, J.J. Watkins, Deposition of gold films and nanostructures from supercritical carbon dioxide. Chem. Mater. **16**, 2028–2033 (2004)
18. B. Zhao, T. Momose, T. Ohkubo, Y. Shimogaki, Acetone-assisted deposition of silver films in supercritical carbon dioxide. Microelectron. Eng. **85**, 675–681 (2008)
19. H. Kim, T. Koseki, T. Ohba, T. Ohta, Y. Kojima, H. Sato, Y. Shimogaki, Cu wettability and diffusion barrier property of Ru thin film for Cu metallization. J. Electrochem. Soc. **152**, G594–G600 (2005)
20. T. Momose, T. Uejima, H. Yamada, Y. Shimogaki, M. Sugiyama, Ultra-conformal metal coating on high-aspect-ratio three-dimensional structures using supercritical fluid: controlled selectivity/non-selectivity. Jpn. J. Appl. Phys. **51**, 056502–056505 (2012)
21. Sigma-Aldrich, Bis(pentamethylcyclopentadienyl) manganese(II)-Material Safety Data Sheet (2012). [Online] Available at: http://www.sigmaaldrich.com/catalog/product/aldrich/415405
22. W. Steinhogl, G. Schindler, G. Steinlesberger, M. Traving, M. Engelhardt, Comprehensive study of the resistivity of copper wires with lateral dimensions of 100 nm and smaller. J. Appl. Phys. **97**, 023706–023707 (2005)
23. T. Momose, M. Sugiyama, Y. Shimogaki, In situ observation of initial nucleation and growth processes in supercritical fluid deposition of copper. Jpn. J. Appl. Phys. **47**, 885 (2008)